Capacity, fragility and damage in reinforced concrete buildings. A probabilistic approach.

Yeudy F. Vargas, Luis G. Pujades, Alex H. Barbat and Jorge E. Hurtado.

Yeudy F. Vargas

Polytechnic University of Catalonia, BarcelonaTech.

Luis G. Pujades *(corresponding author)*

Polytechnic University of Catalonia, BarcelonaTech.

Jordi Girona 1-3, D2

08034 Barcelona (Spain)

Tel.: +34-934017258

Fax: +34-934017251

E-mail: lluis.pujades@upc.edu

Alex H. Barbat

Polytechnic University of Catalonia, BarcelonaTech.

Jorge E. Hurtado

Universidad Nacional de Colombia, Sede Manizales.

Abstract

The main goals of this article are to analyze the use of simplified deterministic nonlinear static procedures for assessing the seismic response of buildings and to evaluate the influence that the uncertainties in the mechanical properties of the materials and in the features of the seismic actions have in the uncertainties of the structural response. A reinforced concrete building is used as a guiding case study. In the calculation of the expected spectral displacement, deterministic nonlinear static methods are simple and straightforward. For not severe earthquakes these approaches lead to somewhat conservative but adequate results when compared to more sophisticated procedures involving nonlinear dynamic analyses. Concerning the probabilistic assessment, the strength properties of the materials, concrete and steel, and the seismic action are considered as random variables. The Monte Carlo method is then used to analyze the structural response of the building. The obtained results show that significant uncertainties are expected; uncertainties in the structural response increase with the severity of the seismic actions. The major influence in the randomness of the structural response comes from the randomness of the seismic action. A useful example for selected earthquake scenarios is used to illustrate the applicability of the probabilistic approach for assessing expected damage and risk. An important conclusion of this work is the need of broaching the fragility of the buildings and expected damage assessment issues from a probabilistic perspective.

Keywords *Capacity, fragility, seismic damage, reinforced concrete buildings, probabilistic.*

1 Introduction

More than two thousand years ago, Vitruvius (1 BC) already stated that architecture is the merging of functionality, strength and beauty. Since the last decade of the twentieth century, the performance based design is an important engineering outcome, becoming a sign of the advances in building construction that concerns mainly to functionality and strength (SEAOC Vision 2000 Committee, 1995). In the case of earthquakes, the capacity spectrum method (Freeman et al. 1975, Freeman 1978, 1998) allows to characterize the interaction between the seismic demand and the building. Simplified procedures enable determining the displacement demand imposed on a building expected to deform inelastically (ATC, 1996; FEMA, 1997). For seismic risk analysis several simplified methods have been developed too. Expert opinion based methods (ATC, 1985; 1991) and vulnerability index based methods (Barbat et al. 1996; 1998) define the earthquake by means of macroseismic intensities (Grünthal, 1998). Capacity spectrum based methods (CSBM) have been adopted too for assessing the seismic risk of existing buildings (FEMA, 1999; McGuire, 2004). CSBM define the building by means of capacity curve, obtained by using Pushover Analysis (PA), while the earthquake is defined by the 5% damped elastic response spectrum. When the response of the structure is dominated by the fundamental mode of vibration, the capacity curve can be expressed in the Acceleration Displacement Response Spectrum (ADRS) format. These spectral values define the so called capacity spectra (Fajfar, 1999) also named capacity diagrams (Chopra and Goel, 1999). The intersection of capacity and demand spectra provides an estimate of the inelastic acceleration and displacement demand (Fajfar, 1999). In CSBM vulnerability is defined by fragility curves. Simplified procedures allow obtaining fragility curves from capacity spectra (Lagomarsino and Giovinazzi, 2006). These simplified procedures have been applied to different building types and cities (see for instance Barbat et al. 2008; Lantada et al. 2009; Pujades et al. 2012). However, all these risk studies are deterministic in the sense that they do not take into account the uncertainties, neither epistemic nor aleatory, of the parameters involved. Nonlinear Dynamic

Analysis (NLDA) consists in subjecting the structure to acceleration time-histories, which can be defined by synthetic or recorded accelerograms. This more sophisticated and costly structural analysis allows to calculate the time-histories of the structural response, being frequently used for comparison between the maximum values and the ones coming from more straightforward static methods (Mwafy and Elnashai, 2001; Poursha et al. 2007; Kim and Kuruma, 2008). It is worth noting that in these works the problem neither is faced from a probabilistic viewpoint. Among many others authors, McGuire (2004) emphasizes the importance of dealing with the seismic risk assessment from a probabilistic point of view. Actually there are many sources of randomness due to aleatory and epistemic uncertainties. A number of issues concerning the impact of epistemic uncertainties on earthquake loss models are described and discussed in Crowley et al. (2005). Most of the parameters involved in the assessment of seismic risk of structures are random variables. Concerning the structure itself, a few examples are the parameters related to the characteristics of the materials, geometry and size of the structure and of the cross sections of its structural elements, cracking and crushing of concrete, strain hardening and ultimate strength of steel, and many others. Moreover, a significant source of randomness is the expected seismic action. So, effective peak acceleration, peak ground acceleration (PGA), frequency content and duration are random variables that introduce significant uncertainties in the structural response. To overcome this high variability in a deterministic, simplified, way, seismic design standards suggest using decreased material strengths and increased seismic actions. However, it is well known that in a nonlinear system it is not assured that a variation in the input parameters would produce a similar variation in the output parameters. Thus, increasing the severity of the expected seismic actions and decreasing strength parameters do not assure the reliability of the response. Besides, these conservative assumptions may lead to excessively conservative responses. Therefore, we conclude that it is necessary to face structural analysis and seismic risk assessment by using probabilistic approaches. Borzi et al. (2008) treat the strength parameters and dimensions of structural capacity as being random. Fragiadakis and Vamvatsikos (2010) evaluate the nonlinear behavior of structures by means of NonLinear Static Analysis (NLSA). They took into account the uncertainties of the properties of the materials, by using a Monte Carlo procedure. Dolsek (2009) considered the

randomness of the seismic action using accelerograms of real earthquakes compatible with target design spectra, but did not take into account the uncertainties of the mechanical properties of the structure. The main goals of this article are the following: (1) the analysis of the use of NLSA for assessing the seismic response of buildings when compared to NLDA; (2) to analyze the influence of the uncertainties in the structural response produced by the uncertainties in the structural properties and in the seismic actions. Concerning structural properties, for simplicity, only the randomness of the steel yield strength and the concrete compressive strength are considered. The uncertainties in the seismic actions are considered by means of sets of accelerograms corresponding to real earthquakes whose response spectra fit well the design spectra chosen for the analysis. A reinforced concrete building is used as a guiding case study. A simplified CSBM is used to assess the fragility and expected damage of this building. The seismic response is also investigated by means of NLDA. Both analyses, static and dynamic, are carried out by means of deterministic and probabilistic approaches. The Ruaumoko software (Carr, 2000) is used for the computations involved in the structural analyses. The results are then used for comparison and discussion.

2 Building and building model

The building has a reinforced concrete building with waffle slabs. This type of building is frequently used in Spain, being well known its limited ductility (Vielma et al. 2009; 2010). The building has 8 stories and 6 spans (Fig. 1). Some details of the construction of waffle slabs can be seen in Fig. 1 too. However, in the computational model, waffle slabs are approximated by beams with equivalent cross sectional inertia. Moreover, it is assumed that beams and columns follow the Takeda hysteretic rule (Otani, 1974). Yield surfaces are defined by the interaction diagram of bending moment and axial force of the columns and bending moment curvature in beams. Loads are applied following the recommendations of Eurocode 8 (EC8, 2004) for reinforced concrete structures. The Rayleigh or proportional damping model is used. The concrete compressive strength, f_c, and the steel yield strength, f_y, are modeled as normal random variables. Table 1 shows the corresponding mean, μ, standard deviation, σ, and coefficient of

variation, *c.o.v.* For deterministic approaches, design standards suggest using characteristic values for the strength of the materials. The characteristic value is defined as the one having an exceedance probability equal to 0.95. For normal probability distributions, the following equations define the characteristic values, $f_c^{'}$ and $f_y^{'}$ of f_c and f_y respectively.

$$f_c^{'} = \mu_{f_c} - 1.65\,\sigma_{f_c}$$
$$f_y^{'} = \mu_{f_y} - 1.65\,\sigma_{f_y} \qquad (1)$$

Table 1 shows the characteristic values, which have been used in the deterministic approach. Normal probability distributions have been assumed.

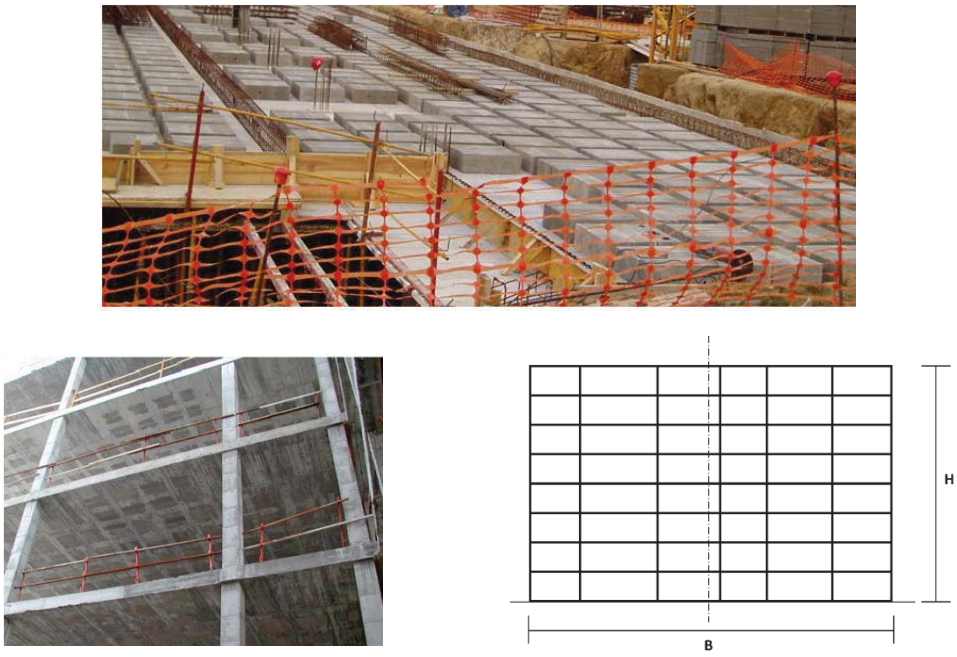

Fig. 1 Waffle slab construction details and building model (down right). The main dimensions are: H = 25.65 m, B = 24 m and the fundamental period is T=1.44 s.

Table 1 Mean values, μ, standard deviations, σ, coefficients of variation, *c.o.v.* and characteristic values of f_c and f_y as normal random variables.

	μ (*MPa*)	σ (*MPa*)	Coefficient of variation (*c.o.v.*)	Characteristic values (*kPa*)	
f_c	30	1.5	0.05	$f_c^{'}$	27525
f_y	420	21	0.05	$f_y^{'}$	385350

These characteristic values have been used in the deterministic approach, while the normal probability distributions defined by the parameters of Table 1 have been used in the probabilistic approach based on Monte Carlo simulations.

3 Seismic actions

NLSA requires defining the seismic actions by means of 5% damped elastic response spectra; NLDA requires acceleration time histories. The 5% damped elastic response spectra provided in the Eurocode EC8 are considered in the analysis and a wide range of PGA is used in such a way that the structural response can be analyzed in the range between the elastic behavior and the collapse. The comparison of the results of NLDA requires that accelerograms be compatible with the response spectra used in NLSA. There are several ways to tackle this issue. One solution is to use synthetic accelerograms (Gasparini and Vanmarcke, 1976) compatible with the response spectrum. Other option is to use real accelerograms. Hancock et al. (2008) provide an overview of the different approaches based on real accelerograms. The choice is not straightforward as there are many legitimate options between these two alternatives. Anyhow, for seismic damage and risk assessment, Faccioli (2006) and Faccioli and Pessina (2003) recommend the use of accelerograms of actual earthquakes and this choice has been preferred in this work. A specific method for the selection of the optimum number of accelerograms from a given database compatible with a given response spectrum is proposed in this paper. This method is described in the Appendix. The spectra provided in the EC8 are considered in this study. These spectra will be referred as 1A, 1B, 1C, 1D, 2A, 2B, 2C and 2D, where the number stands for the spectrum type (1 for magnitudes M > 5.5), and the letter for the soil type. The normalized spectral shapes are shown in Fig. 2. The extreme spectra 1A, 1D, 2A and 2D have been highlighted. These four spectra will be used in NLSA. For the vibration period of the building (T=1.44 s) the 1D spectrum has the highest response and the 2D spectrum is a little bit higher than the 1A spectrum. NLSA and NLDA confirm that the spectral displacements and expected damage are greater for seismic actions defined by the 1D and 2D spectra. Moreover, the spectral displacement of the ultimate point of the capacity spectrum of the building considered is 21 cm. To get this ultimate spectral displacement by using seismic actions defined by the other spectra of Fig. 2, it would be necessary to scale accelerograms to PGA values greater than 0.6 g, that are unlikely in Spain, where the PGA for a return period of 500 years is less than 0.25g (NCSE-02, 2002).

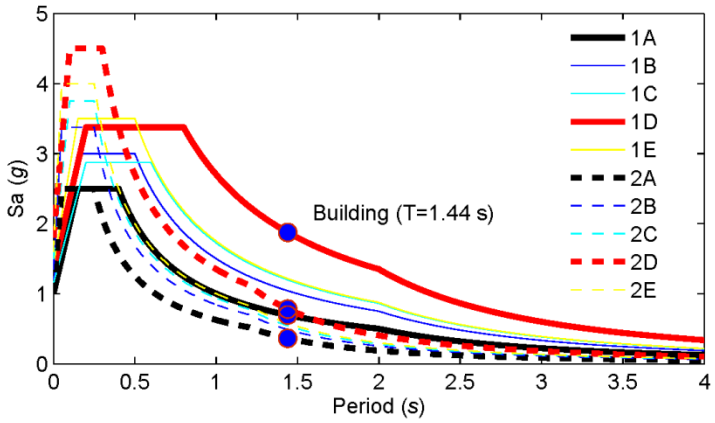

Fig. 2 Normalized EC8 5% damped elastic response spectra. Markers correspond to the fundamental period of the building.

Therefore, in this paper NLDA, both probabilistic and deterministic, is performed using only accelerograms matching the 1D spectrum. This analysis has been considered sufficient for the purpose of this work. NLDA is carried out by means of the Incremental Dynamic Analysis (IDA) as proposed by Vamvatsikos and Cornell (2001).

4 Deterministic approach

The capacity, fragility and expected damage are first estimated by means of deterministic NLSA and NLDA approaches.

4.1 Deterministic approach

For deterministic PA, characteristic values are used. The loading pattern (triangular, rectangular, and so on) has a major influence on the results (Mwafy and Elnashai, 2001). The Adaptive Pushover Analysis (APA) technique proposed by Satyarno (1999) has been used in this work. A detailed description of this procedure can be found in the Ruaumoko software manuals (Carr, 2000). Fig. 3a shows the capacity curve and Fig. 3b shows the capacity spectrum (see also Mata et al. 2007; Faleiro et al. 2008) and its bilinear simplified form (ATC 1996), which is defined by the yielding point (*Dy*, *Ay*) and the ultimate capacity point (*Du*, A*u*). In this case, *Dy*=13 cm, A*y*=0.23 g, *Du*=21 cm and *Au*=0.24 g. *Dy* and *Du* are used for constructing fragility curves by means of a simplified procedure.

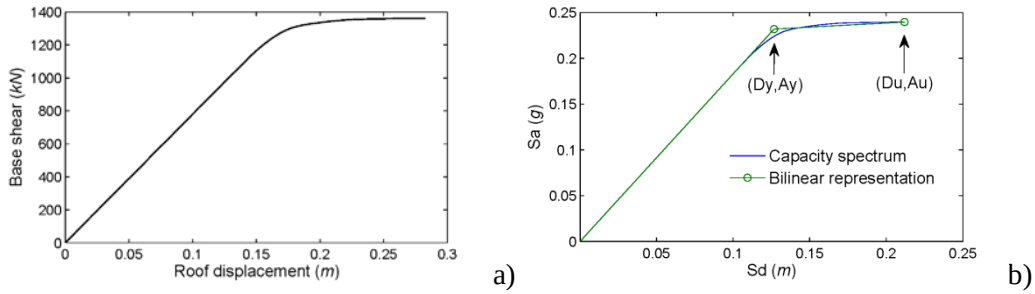

Fig. 3 Capacity curve (a) and capacity spectrum (b) obtained from the deterministic APA.

For a given damage state, ds_i , the fragility curve defines the probability that ds_i be equaled or exceeded as a function of a parameter defining the intensity of the seismic action (FEMA, 1999). The following equation defines the fragility curve as a function of Sd :

$$P\left[d \geq ds_i \left| Sd \right. \right] = \varphi \left[\frac{1}{\beta_{ds_i}} ln\left(\frac{Sd}{\overline{Sd}_{ds_i}} \right) \right] \qquad (2)$$

where φ stands for the cumulative lognormal distribution, d is the expected damage, Sd is the spectral displacement and $\overline{Sd}_{ds_i}$ and β_{ds_i} are the median values and standard deviations of the corresponding normal distributions. For simplicity we call $\overline{Sd}_{ds_i}$ as μ_i and β_{ds_i} as β_i . μ_i is also called damage state threshold, and the probability of exceedance of the damage state ds_i for $Sd = \mu_i$ is equal to 0.5. The following simplified assumptions allow obtaining fragility curves from the bilinear form of the capacity spectrum. 1) μ_i are related to the yielding and ultimate capacity points as follows:

$$\mu_1 = 0.7Dy, \quad \mu_2 = Dy, \quad \mu_3 = Dy + 0.25\,(Du - Dy), \quad \text{and } \mu_4 = Du \qquad (3)$$

and 2) the expected seismic damage follows a binomial probability distribution. These assumptions were proposed in the framework of the Risk-UE project (Risk-UE, 2004; Milutinovic and Trendafiloski, 2003; Lagomarsino and Giovinazzi, 2006) and have been used in many seismic risk studies for European earthquake prone cities (see for instance Barbat el al. 2008; Pujades et al. 2012). The first assumption is based on expert opinion and relates the expected damage to the stiffness degradation of the structure; the second one is based on the damage observed in past earthquakes (Grünthal, 1998). A detailed description on how μ_i and β_i are obtained can be found in Lantada et al. (2009). Fig.4a shows the fragility curves. Markers indicate the points obtained applying the two simplifying

assumptions described above. Table 2 shows the values of μ_i and β_i. The performance point defines the spectral displacement, Sd_p, that a seismic action will produce in the building. Once this spectral displacement is known, fragility curves allow assessing the probabilities of exceedance of each damage state and, therefore, the probabilities of occurrence of each damage state, or Damage Probability Matrices (DPM), can be easily known. Furthermore, a damage index is defined and used to represent the expected damage by means of only one parameter. Methods for obtaining the performance point use Capacity-Demand-Diagrams which are based on inelastic response spectra in ADRS format (Mahaney et al. 1993; ATC 1996). Although several improvements of the ATC-40 (ATC, 1996) methods have been proposed (see for instance Chopra and Goel, 1999), for the purpose of this work, two well-known simplified procedures have been used. The first one is the Equal Displacement Approximation (EDA). The second method, known as Procedure A in the chapter 8 (PA-8) of ATC-40, involves an iterative process. The capacity spectrum method based on inelastic demand spectra was rigorously tested by Fajfar (1999), who concluded that it provides a good approximation for the spectral displacement of a structure taking into account its nonlinear behavior. Both procedures have been applied to the 1A, 1D, 2A and 2D spectra for increasing PGA between 0.01 and 1.6 g. Fig. 4b shows the spectral displacements as functions of the PGA. 1D response spectrum is the most demanding one, while 2A spectrum is the less demanding one. Let ds_i $(i = 1 \cdots 4)$ be the four non-null damage states. Let P_i be the probability of occurrence of the damage state ds_i. $i = 0$ corresponds to the *no-damage* or *null* damage state; $i = 1,2,3,4$ respectively corresponds to *Slight*, *Moderate*, *Severe* and *Complete* damage states. Then $P_i(Sd)$ values can be computed in the following way:

$$\begin{aligned} P_0(Sd) &= 1 - P\left[d \geq ds_1 \middle| Sd \right] \\ P_i(Sd) &= P\left[d \geq ds_i \middle| Sd \right] - P\left[d \geq ds_{i+1} \middle| Sd \right] \quad i = 1 \cdots 3 \\ P_4(Sd) &= P\left[d \geq ds_4 \middle| Sd \right] \end{aligned} \tag{4}$$

where $P\left[d \geq ds_{i+1} \middle| Sd \right]$ values, at the right site of these equations, can be obtained by using equation (2).

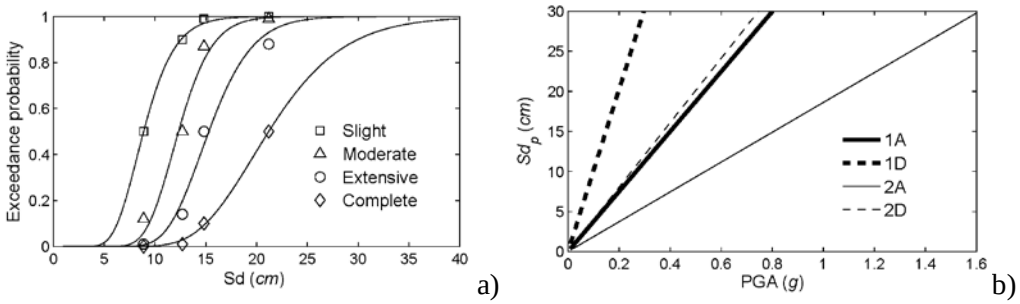

Fig. 4 a) Deterministic fragility curves. b) Spectral displacements, Sd_p, obtained by using the EDA method for 1A, 1D, 2A and 2D EC8 response spectra.

Table 2 Parameters μ_i and β_i for the deterministic fragility curves.

	Non-null damage states			
	1) *Slight*	2) *Moderate*	3) *Severe*	4) *Collapse*
μ_i (cm)	8.9	12.3	15.3	21.2
β_i	0.27	0.21	0.22	0.27

It is useful to define the following damage index that can be understood as the mean damage grade:

$$di(Sd) = \sum_{i=0}^{4} iP_i(Sd) \tag{5}$$

$di(Sd)$ takes values between 0 and 4. $di(Sd) = 0$ means that the probability of the *no-damage* is equal to 1 and $di(Sd) = 4$ means that the probability of the *Complete* damage state or *Collapse* is equal to 1. Moreover, it is well known that the binomial distribution is controlled by only one parameter taking values between 0 and 1. In our case this parameter is $DI(Sd) = di(Sd)/4$, being 4 the number of non-null damage states. $DI(Sd)$ completely defines the P_i values and, using equations (4), these values completely define the fragility curves. Furthermore, taking into account that for a given seismic action there is a relation between Sd_p and PGA (see Fig. 4b), fragility curves and damage functions can be also represented as functions of PGA. Fig. 5a shows the damage functions for seismic actions defined by the 1A, 1D, 2A and 2D response spectra. In this figure a PGA value of 0.4 g has been chosen to illustrate the computation of DPM, *di* and *DI*. Table 3 shows the results obtained. Fig. 5b shows the corresponding DPM.

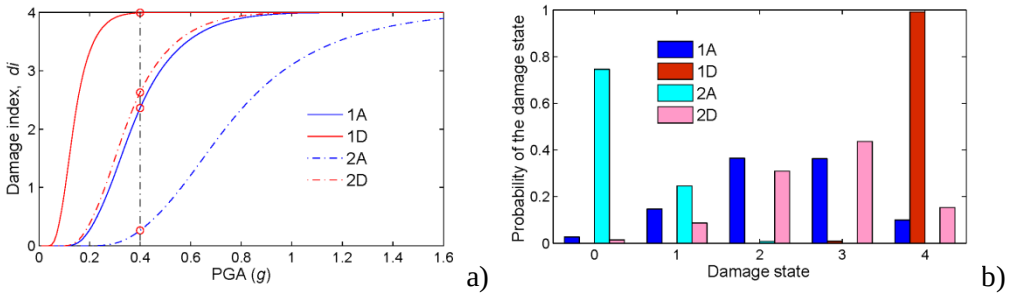

Fig. 5 a) Damage index, *di* , for seismic actions defined by EC8 1A, 1D, 2A and 2D spectra. b) Corresponding DPM for PGA=0.4 g.

Table 3 DPM, P_i, and damage indices *di* and *DI* for PGA=0.4 g.

EC8 spectrum	Probabilities of the damage states					*di*	*DI*
	0) *No-damage*	1) *Slight*	2) *Moderate*	3) *Severe*	4) *Collapse*		
	P_0	P_1	P_2	P_3	P_4		
1A	0.03	0.15	0.36	0.36	0.10	2.36	0.59
1D	***	***	***	0.01	0.99	3.99	1.00
2A	0.74	0.25	0.01	***	***	0.26	0.07
2D	0.01	0.09	0.31	0.44	0.15	2.63	0.66

(***) means very low probability

4.2 Nonlinear dynamic analysis

As pointed out above, IDA is performed using only records compatible with the 1D spectrum. Moreover, in the NLSA using EDA and PA-8 approaches for the 1D spectrum, the PGA needed for reaching the extreme case of collapse is about 0.3 g (see Fig. 5). Thus, the accelerograms compatible with the 1D spectrum will be scaled between 0.06 and 0.36 g, by increments of 0.06 g. Vamvatsikos and Cornell (2001) performed an interesting analogy between PA and IDA, showing how both procedures increase the loads applied to the structure and measure the response of the system in terms of a control variable, which can be the displacement at the roof or the maximum inter-story drift, among others. Thus, IDA allows also obtaining a relationship between PGA and Sd_p. But, to estimate this deterministic relationship only one accelerogram is needed. This accelerogram has been obtained according to the following procedure. From the mean spectrum and its standard deviation, calculated over the 20 actual spectra, which will be used in the probabilistic NLDA, a characteristic spectrum is defined as that having a 5% likelihood of being exceeded. This spectrum is shown in Fig. 6a. Then, a compatible artificial accelerogram is generated after this characteristic spectrum. The choice of an artificial accelerogram has been preferred because it

optimizes the matching to the target spectrum. The algorithm proposed by Gasparini and Vanmarcke (1976) is used for this purpose, with the trapezoidal envelope proposed by Hou (1968). The duration of the simulated earthquake was defined as the average duration of the 20 accelerograms used in the probabilistic NLDA. Other ways for considering the duration is discussed by Hancock and Bommer (2006). Fig. 6b shows the results obtained by applying deterministic EDA, PA-8 and NLDA approaches.

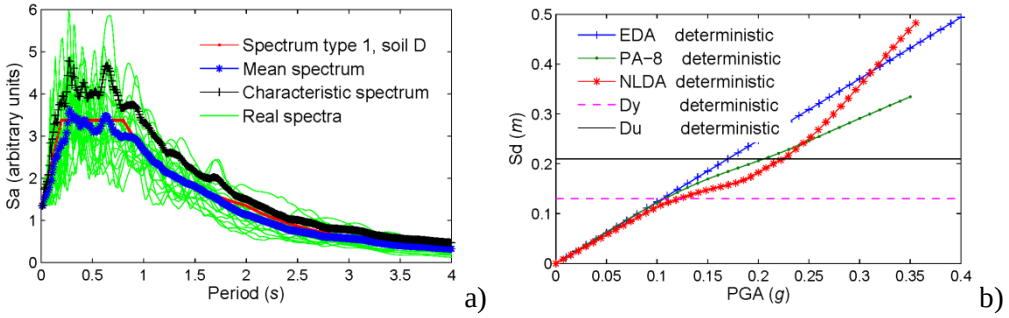

Fig. 6 a) Characteristic spectrum obtained from real accelerograms. b) Results of the deterministic approach.

Yielding, *Dy*, and ultimate, *Du*, capacity spectral displacements are also plotted in this figure. In our view, for PGA values higher than the corresponding to *Du*, the results have little or no sense. For lower PGA values simplified procedures are conservative but there is a better agreement between spectral displacements obtained by using PA-8 and NLDA approaches.

5 Probabilistic approach

The capacity, fragility and expected damage are now estimated by means of probabilistic NLSA and NLDA approaches. This way, the deterministic and probabilistic results can be compared. Furthermore, the probabilistic approach allows analyzing the influence of the variability of the input parameters upon the structural response and performance of the building.

5.1 Nonlinear static analysis

NLSA has been carried out 10 000 times. The values of f_c and f_y as Gaussian random variables have been shown in Table 1. The 56 columns of the building (Fig. 1) are divided into eight groups, each group corresponding to a storey. The correlation matrix is used to take into account the correlation among the samples.

Thus, high correlation is considered among the samples generated for the columns belonging to a same group, but the correlation among the samples of different groups is considered to be null. This way, a kind of spatial variability of the randomness is also taken into account. The same approach is used with the beams. The columns are attached to waffle slabs that are modeled by beams having equivalent cross sectional inertia. Since the floors are alike in all levels, there is only one type of cross section for these beams. In each repetition of the Monte Carlo technique, for each element, column or beam, of one group, a random sample of concrete and steel strength is generated, according to the procedure described in Kalos and Whitlock (1986). Fig. 7 shows the 10 000 capacity curves, the mean capacity curve and the deterministic capacity curve obtained using characteristic strength values. It is worth noting that the maximum displacement value of the deterministic curve is exceeded by 82.5% of all the capacity curves.

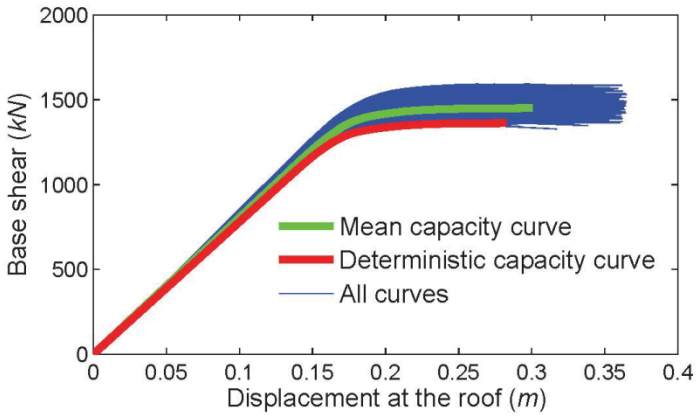

Fig. 7 Mean and individual capacity curves obtained in the probabilistic approach. The deterministic capacity curve is also shown.

So, the probability that the structure reaches the collapse before this value is 17.5%. Furthermore, key parameters of the capacity curves coming from the Monte Carlo simulations are random too. Fig. 8 shows the correlation plots between K_0 and f_c, and between δ_u and f_y. It can be seen how δ_u slightly increases with f_y (Fig. 8a). Fig. 8b shows that there is a strong dependence between K_0 and f_c. In order to have a more accurate measure of the degree of dependence between input and output variables, the correlation matrix has been calculated. The input random variables are f_y and f_c. The output random variables considered herein are K_0, Dy, Du, and q. $q = \frac{Du}{Dy}$ is the ductility capacity factor.

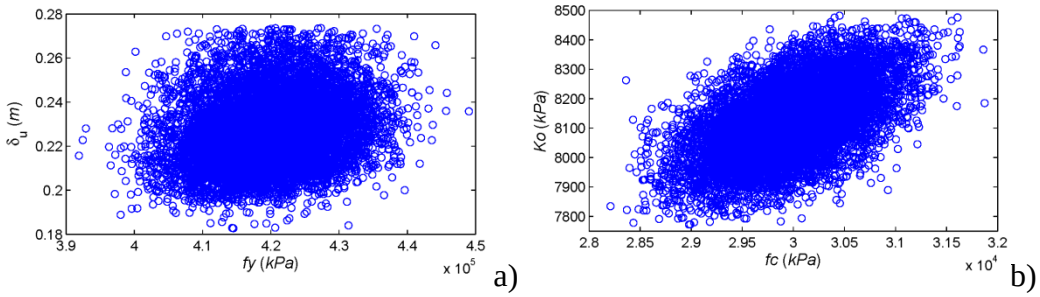

Fig. 8 Correlation between δ_u and f_y (a) and between K_0 and f_c (b).

The correlation matrix, ρ_{ij}, can be calculated using the following equation:

$$\rho_{ij} = \frac{Cov(x_i, x_j)}{\sigma_{x_i}\sigma_{x_j}} \tag{6}$$

where x_i and x_j are variables, Cov is their covariance, and σ_{x_i} and σ_{x_j} are the standard deviations of the variables x_i and x_j. The correlation matrix is shown in Table 4.

Table 4. Correlation matrix between the random variables.

		Input variables		Output variables			
		f_y	f_c	q	K_0	Dy	Du
Input variables	f_y	1.00	0.00	0.13	-0.01	0.34	0.21
	f_c	0.00	1.00	-0.14	**0.55**	0.18	-0.10
Output variables	q	0.13	-0.14	1.00	-0.48	-0.20	**0.97**
	K_0	-0.01	**0.55**	-0.48	1.00	**0.71**	-0.33
	Dy	0.34	0.18	-0.20	**0.71**	1.00	0.03
	Du	0.21	-0.10	**0.97**	-0.32	0.03	1.00

As expected, a strong correlation value of 0.71 exists between stiffness and yielding spectral displacement and a value of 0.97 between ductility and ultimate spectral displacement. Significant correlation values of 0.55 between K_0 and f_c and of 0.34 between f_y and Dy can be seen too. The correlation analysis shows the wealth of information that can be obtained from probabilistic approaches.

Equations (3) allow computing the damage states thresholds for each one of the capacity curves of Fig. 7. Fig. 9 shows these damage states thresholds, ds_i, together with the corresponding to the deterministic capacity curve. Table 5 shows mean values, μ_{ds_i}, standard deviations, σ_{ds_i}, and coefficients of variation, $c.o.v$. Deterministic damage state thresholds, $ds_{i,\text{det}}$, are also shown in Table 5 and in

Fig. 9. It can be observed that ds_1 and ds_2 are strongly correlated with the spectral acceleration because the corresponding spectral displacements are near the zone where the behavior of the building is linear.

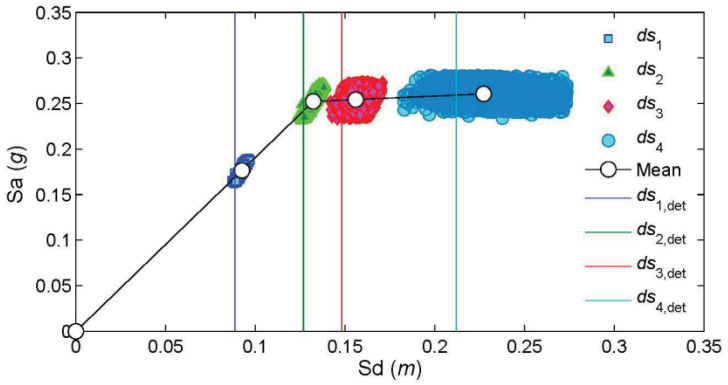

Fig. 9 Damage states thresholds obtained with the probabilistic and deterministic approaches.

However ds_3 and especially ds_4 exhibit much more dispersion. Note that dispersion increases with increasing spectral displacements. Thus the probability that ds_i, be inferior to the $ds_{i,\det}$, also increases. Table 5 also shows the values of these probabilities $P[ds_i < ds_{i,\det}]$.

Table 5 Mean values, standard deviations and coefficients of variation *c.o.v.* of the damage state thresholds. The deterministic values and the probability, that ds_i, obtained with the probabilistic method, be inferior to $ds_{i,\det}$, estimated with the deterministic procedure, $P[ds_{i_i} < ds_{i,\det}]$, are also shown.

	Damage states			
	1) *Slight*	2) *Moderate*	3) *Extensive*	4) *Collapse*
Mean values μ_{ds_i} (cm)	9.2	13.2	15.6	22.7
Standard deviations σ_{ds_i} (cm)	0.16	0.22	0.51	1.60
Coefficients of variation *c.o.v*	0.02	0.02	0.03	0.07
Deterministic values $ds_{i,\det}$ (cm)	8.8	12.7	14.8	21.2
Probability $P[ds_i < ds_{i,\det}]$	0.004	0.004	0.029	0.175

Fragility curves are completely defined should ds_i and β_i be known. As explained above, these parameters can easily be estimated from bilinear capacity spectra and simplifying assumptions. Fig. 10a shows the fragility curves. Again, the variability increases with increasing damage states. Note that this increase is due to the increasing nonlinearity of the structural response. Fig. 10b plots the ds_i

median values of the lognormal function against the corresponding β_i, illustrating the correlation between ds_i and β_i.

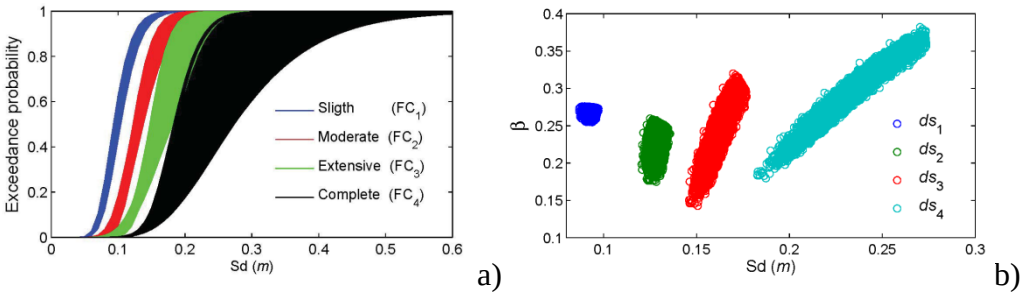

Fig. 10 Fragility curves obtained with the probabilistic approach (a), and correlation among the parameters ds_i and β_i defining the lognormal functions of the fragility curves (b).

Table 6 shows the correlation coefficients, which also increase as ds_i increases. In order to represent the probabilistic fragility curves in a parametric form, a Gaussian model for the parameters describing the fragility curves has been tested.

Table 6 Correlation coefficients between ds_i and β_i.

	$ds_1 - \beta_1$	$ds_2 - \beta_2$	$ds_3 - \beta_3$	$ds_4 - \beta_4$
ρ_{ii}	-0.20	-0.20	0.82	0.97

Fig. 11 shows the comparison of the empirical and parametric models for ds_i, showing a good fit.

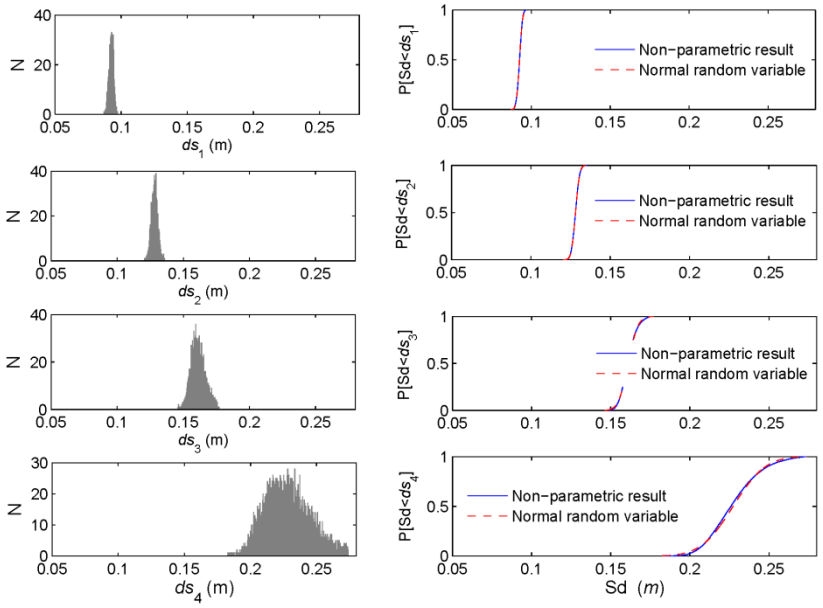

Fig. 11 Histograms and comparison with Gaussian random distributions for ds_i.

Similar results have been obtained for β_i . Table 7 shows the mean values, standard deviations and coefficients of variation of the Gaussian models.

Table 7 Mean values μ , standard deviations σ and coefficients of variation, *c.o.v.*, of the random variables that define the fragility curves.

	Damage states							
	1) *Slight*		2) *Moderate*		3) *Extensive*		4) *Collapse*	
	ds_1 (cm)	β_{ds_1}	ds_2 (cm)	β_{ds_2}	ds_3 (cm)	β_{ds_3}	ds_4 (cm)	β_{ds_4}
μ	9.2	0.27	12.8	0.218	16.1	0.231	22.7	0.28
σ	0.2	0.004	0.2	0.015	0.5	0.03	1.6	0.035
c.o.v	0.022	0.015	0.016	0.069	0.031	0.130	0.070	0.125

Thus, it is possible to estimate these parameters and, consequently, the fragility curves for any confidence level. Another equivalent way of analyzing the results of the Monte Carlo simulation is the following: for each spectral displacement and for each set of fragility curves in Fig. 10a, the mean value, the 95% confidence level and the standard deviation can be obtained. Fig. 12a shows the mean and the 95% confidence level fragility curves, together with the deterministic fragility curves. Fig.12b shows the standard deviation of each fragility curve as a function of the spectral displacement.

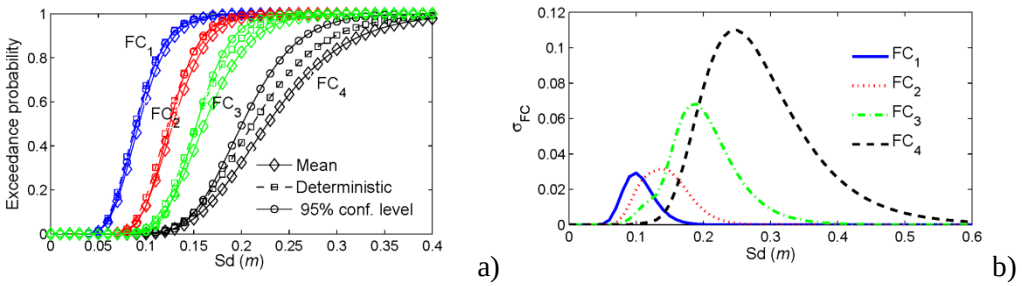

a) b)

Fig. 12 Mean fragility curves obtained with the probabilistic approach. The 95% confidence level and the deterministic fragility curves are also shown (a). Standard deviation of the probabilistic fragility curves (b).

It is worth noting that the 95% confidence level fragility curves are greater than the deterministic ones. The differences between these curves increase with increasing damage states and at intermediate spectral displacements close to the damage states thresholds. Note also in Fig. 12b that the greatest standard deviations and thus the greatest uncertainties occur around damage states thresholds. Again these uncertainties increase with increasing spectral displacements.

In order to compare NLSA and NLDA results, it is necessary to obtain the relation between PGA and spectral displacement of the performance point, Sd_p. Thus, for each of the four spectrum types considered and for each of the 10 000 capacity curves, the methods to obtain the performance point described above have been applied. Therefore, the spectra of actual accelerograms have been used for NLSA. The fact that response spectra of actual accelerograms in ADRS format are not one-to-one functions complicates the automation of the process, particularly for the PA-8 procedure. Moreover, as $Sd_p(\text{PGA})$ functions are crucial for damage assessment, it is necessary to assess the uncertainties involved. Knowing these uncertainties can be more important for severe earthquakes or when high confidence levels are needed. The standard deviation is a nice measure of the uncertainty. The results obtained with the probabilistic EDA and PA-8 methods are summarized in Fig. 13. EDA results are conservative. Fig. 13a shows the mean Sd_p for the four EC8 spectra considered, Fig. 13b shows the corresponding standard deviations. The standard deviations of the EC8 2A spectrum are higher than the ones of the EC8 1D spectrum. Again, dispersion increases with increasing PGA.

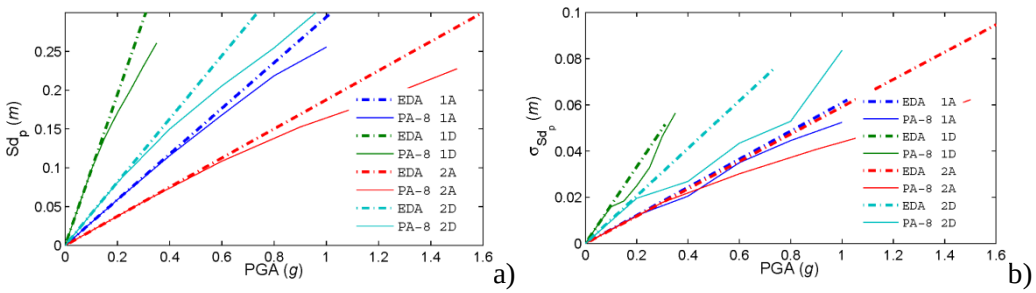

Fig. 13 a) Sd_p obtained with probabilistic EDA and PA-8 techniques. b) Corresponding standard deviations.

Concerning the expected damage, only the EC8 1D spectrum is analyzed. This case will be used for comparison with the IDA probabilistic results. Fig. 14a compares the *DI* obtained by means of the EDA approach and using mean fragility curves, 95% confidence level fragility curves and the deterministic approach using characteristic values. Fig. 14b corresponds to the PA-8 approach. Observe how the deterministic method is a fairly good approach. However, especially for high PGA values, the expected deterministic damage indexes can be slightly lower than the ones corresponding to the 95% confidence level obtained with the probabilistic approach.

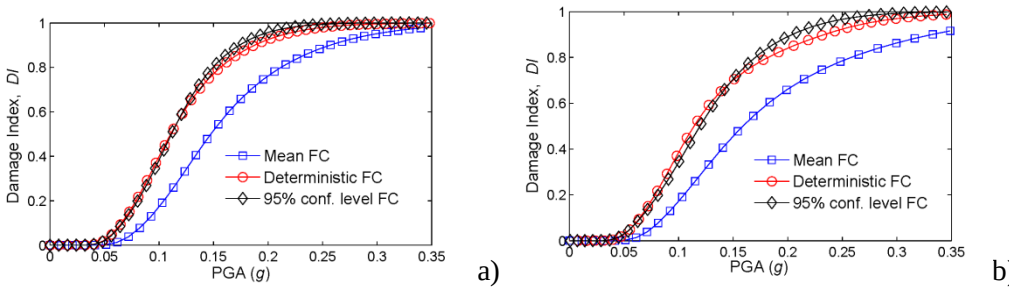

Fig. 14 a) Damage index functions for EC8 1D spectrum: a) EDA procedure and b) PA-8 procedure. In both cases mean, deterministic and 95% confidence level fragility curves (FC) have been used.

Therefore, the use of characteristic values does not assure that the output variables will have the same confidence level than the input ones. Furthermore, as shown in Fig. 13b, significant dispersion is expected.

5.2 Nonlinear dynamic analysis

Now the mechanical properties of materials and the seismic action are considered as random variables. The probabilistic NLDA has been performed also by using the IDA procedure. The twenty accelerograms have been scaled between 0.06 and 0.36 g by increments of 0.06 g. For each of the 20 records only 100 samples of the mechanical properties are generated. This number has been considered sufficient as this implies 2000 NLDA for each of the 6 PGA considered, thus rendering a total of 12000 NLDA. Fig. 15a shows the results obtained. Each color corresponds to a PGA value. For each color, 20 clouds of 100 points are shown. Each cloud corresponds to a real accelerogram and each point corresponds to a sample of the mechanical properties. Note how the dispersions, and indeed the uncertainties, increase with increasing PGA values. Should the results for PGA=0.06 g be closely observed (Fig. 15b), the 20 clouds can be clearly distinguished. For each cloud, the differences are due to the variability of properties of the materials. The differences among different clouds are due to the variability of the 20 accelerograms, thus indicating that an important source of randomness is the seismic action. Similar comments can be said for all the 6 PGA values. It can be also seen in Fig. 15a that as PGA increases, the overall dispersion increases, being more and more difficult to distinguish the 20 clouds. However, the influence of the variability of the seismic action is predominant. Fig. 15c shows the details for the extreme case of PGA=0.36 g.

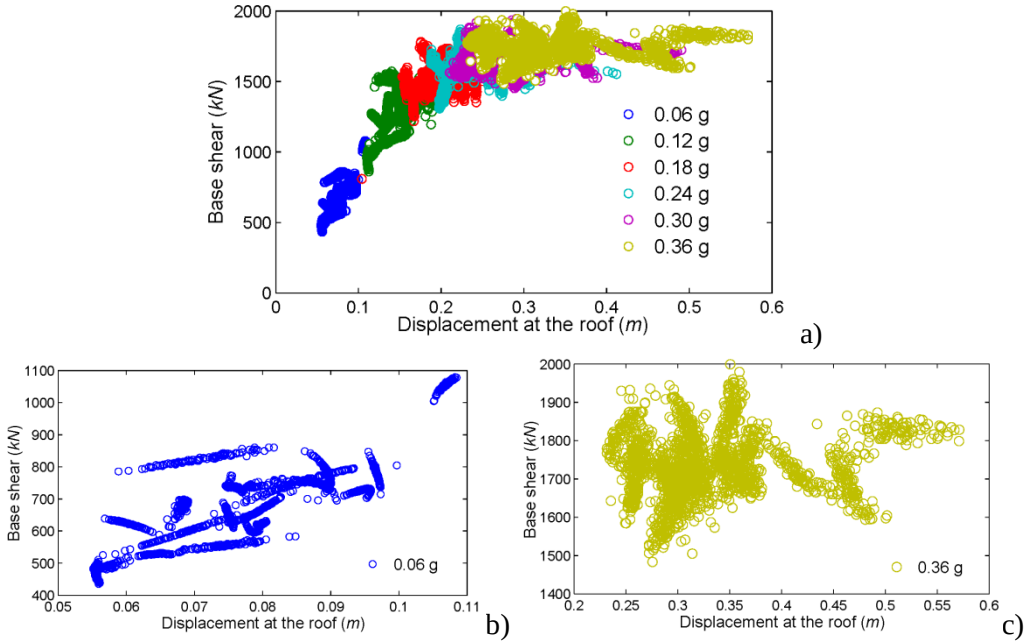

Fig. 15 a) Overall results of probabilistic NLDA. b) Details for PGA = 0.06 g and c) for PGA = 0.36 g c).

This fact is attributed to the growth of the influence of the variability of the mechanical properties of the materials for intense seismic actions as the behavior of the building is governed by the nonlinear response. Thus, the quantitative observation of the great influence of the variability of the seismic actions and of the increasing influence of the variability of the properties of the materials with increasing PGA values is an important outcome of this work. The influence of ground-motion variability in damage and risk calculations has been also described and discussed by Bommer and Crowley (2006). In order to estimate the expected damage, Sd_p values have been computed. Fig. 16a shows Sd_p as a function of the PGA. *Dy* and *Du*, together with their 95% confidence intervals, have been also depicted. Fig. 16b shows the standard deviations of Sd_p. Again, the standard deviations increase with increasing PGA values. Fig. 17 shows the expected *DI*. Mean and 95% confidence curves are shown together with the deterministic case. For intermediate PGA values, the *DI* with a 95% confidence level is greater than the corresponding to the deterministic case. Fig. 17 is similar to Fig.14, where the probabilistic results of applying EDA and PA-8 procedures have been shown. These three cases, EDA, PA-8 and IDA, are compared and discussed in the following section.

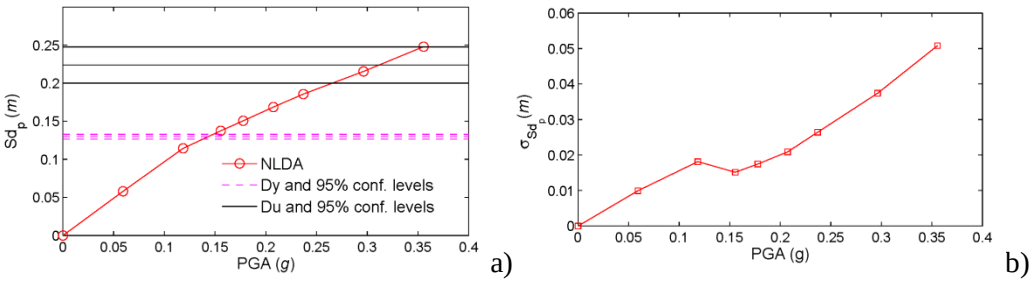

a) b)

Fig. 16 a) Mean Sd_p as a function of PGA. *Dy*, *Du* and the corresponding 95% confidence intervals are also shown. b) Corresponding standard deviations.

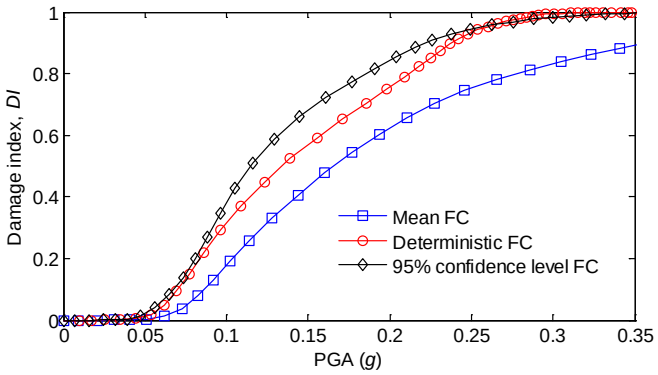

Fig. 17 *DI* as a function of PGA Mean, deterministic and 95% confidence level fragility curves (FC) have been used to assess *DI* .

6 Discussion

In this section the most relevant results of the probabilistic approach are compared and discussed. Moreover, an example of the practical use of probabilistic techniques for assessing the expected seismic damage and risk of actual buildings is presented.

6.1 Comparison of the static and dynamic probabilistic approaches

Fig. 18 summarizes the Sd_p(PGA) functions obtained by means of EDA, PA-8 and IDA probabilistic procedures. Fig. 18a shows the median values and Fig. 18b shows the corresponding standard deviations. For comparison purposes, Fig. 18a also shows *Dy* and *Du* together with their 95% confidence intervals. In both figures, but particularly in Fig. 18b, significant changes in the slopes of the PA-8 and IDA curves can be observed. These changes begin close to *Dy* and they are

attributed to changes in the behavior of the structure when it enters into the nonlinear part of the capacity spectrum that also corresponds to the nonlinear dynamic response (Vargas et al. 2010). It can be seen that the EDA and PA-8 approaches do not underestimate the spectral displacement, when compared to the more realistic procedure IDA, but PA-8 technique gives a more accurate estimation of Sd_p than EDA does.

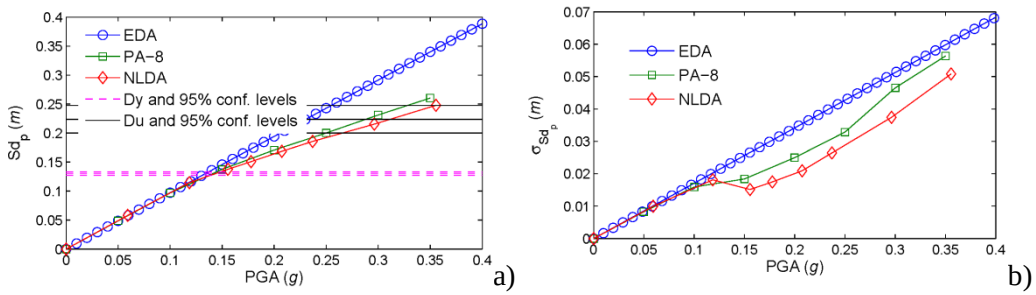

Fig. 18 **a)** Median Sd_p obtained with EDA, PA-8 and NLDA as functions of PGA. *Dy*, *Du* and the corresponding 95% confidence intervals are also plotted. b) Corresponding standard deviations.

Moreover, the greatest standard deviations correspond to the highest PGA values, around and over *Du*. Concerning expected damage, Fig. 19 summarizes the results of the damage index, *DI* , as a function of PGA.

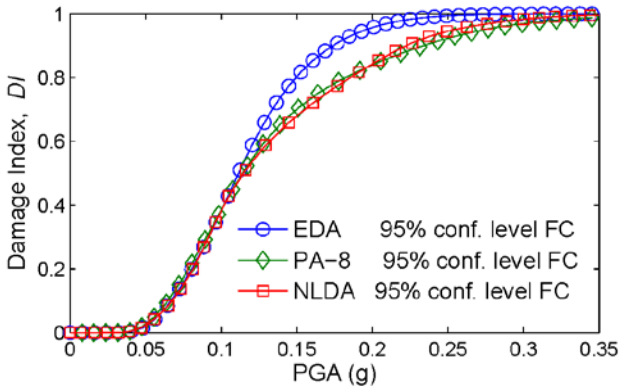

Fig. 19 *DI* as a function of PGA obtained with the EDA, PA-8 and NLDA probabilistic methods. Median Sd_p values and 95% confidence level fragility curves have been used.

In this figure, the Sd_p values of Fig.18a are used together with the corresponding fragility curves at the 95% confidence level. PA-8 and NLDA methods provide similar results. EDA never underestimates the expected damage although, in the range between PGA values of 0.12 and 0.28g, it is somewhat conservative. The corresponding spectral displacements 0.12 and 0.23 m (see Fig. 18a) are close to the damage states thresholds of *Moderate* and *Collapse* damage states (see Fig. 9

and Table 5). The main cause of this effect is attributed to the fact that EDA procedure does not capture the nonlinear behavior of the building.

6.2 Applicability of the probabilistic approach

As said above, most of the seismic risk assessments carried out up to now in urban areas have been performed by using deterministic approaches. The results of these works are usually understood as mean or median expected values. In this section we discuss about the influence that the randomness of the strength properties of the materials and the uncertainty of the seismic action have on the randomness of the expected damage. Moreover, two specific scenarios are analyzed in order to illustrate how the probabilistic results should be understood and how they can be used in practical applications. To do that, Monte Carlo simulations have been performed first, separating the randomness of the mechanical properties of the materials from that of the seismic actions, considering the following three cases: 1) only the mechanical properties are assumed to be random, 2) only the seismic action is assumed to be random and 3) both, the properties of the materials and the seismic action are assumed to be random. These three cases are analyzed by using NLDA. Fig. 20 shows the standard deviation of Sd_p as a function of PGA.

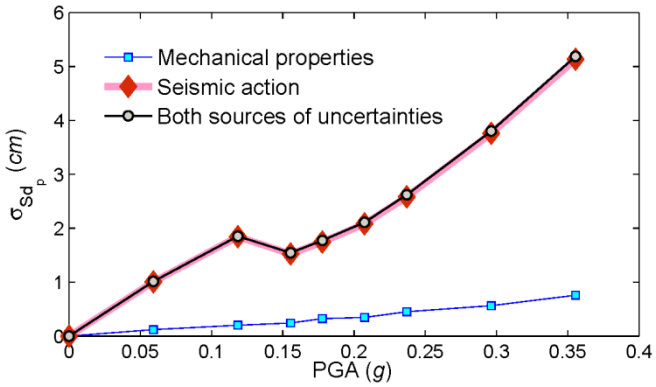

Fig. 20 Standard deviation, σ, of Sd_p, as a function of PGA, considering the randomness of the mechanical properties of the materials, the randomness of the seismic actions and both uncertainties.

It can be seen how the influence of the uncertainties in the mechanical properties of the materials is very low when compared to the influence of the uncertainties in the seismic actions. Uncertainties in the seismic action may have been overestimated due to the insufficiency of the databases of accelerograms used in

this study. Probably these uncertainties can be reduced by using larger and more specific databases. So, in risk assessment studies the uncertainties of the involved parameters should be carefully addressed. One possibility is, for instance, to use logical trees with different reasonable assumptions and weightings in a similar way that it is done in probabilistic seismic hazard analyses (PSHA). It is worth noting that the standard deviations corresponding to the case in which both uncertainties are taken into account can be easily obtained from the quadratic composition of standard deviations, that is:

$$\sigma_T \cong \sigma_Q = \sqrt{\sigma_M^2 + \sigma_A^2} \tag{7}$$

where σ_T is the standard deviation taking into account both uncertainties, σ_M corresponds to the mechanical properties, σ_A corresponds to the seismic action and σ_Q is the quadratic composition of σ_M and σ_A. Table 8 shows selected values of PGA and the corresponding standard deviations taken from Fig. 20. In this table, the standard deviations are compared with the quadratic composition according to equation (7). This result confirms that the seismic actions and the mechanical properties of the materials are independent random variables.

Table 8. Standard deviations in Fig. 20, for PGA values of 0.18 g, 0.24 g and 0.36 g.

PGA (g)	σ_M (cm)	σ_A (cm)	σ_T (cm)	σ_Q (cm)
0.18	0.32	1.74	1.77	1.77
0.24	0.45	2.58	2.62	2.62
0.36	0.76	5.13	5.19	5.19

In order to illustrate the usefulness of the probabilistic approach, two hypothetical earthquake scenarios are considered now. Fig. 21 shows Sd_p as a function of the PGA. The median values and the 95% confidence levels are shown in this figure. The first scenario corresponds to a PGA value of 0.11g; the second one corresponds to a PGA value of 0.24 g. Both scenarios are depicted in Fig. 21 too. To avoid considering the uncertainties twice, in practical applications, special care must be taken. So, to estimate the expected damage we can proceed in one of the two following ways. **Procedure A:** the function $Sd_p(\text{PGA})$ is assumed to be probabilistic and the function $DI(Sd_p)$ is assumed to be deterministic.

Procedure B: $Sd_p(\text{PGA})$ is assumed to be deterministic and $DI(Sd_p)$ is assumed to be probabilistic. In **Procedure A** the uncertainties of the mechanical properties are considered in the capacity curves and, for each PGA, the uncertainties of the

seismic actions are considered in the obtaining of Sd_p; therefore, both uncertainties are included in the resulting Sd_p(PGA) function (see Fig. 21).

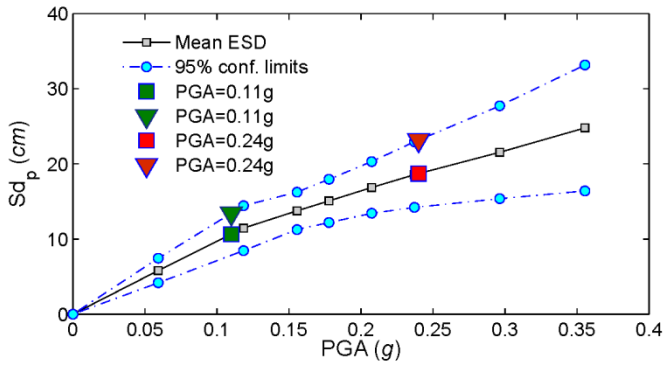

Fig. 21. Sd_p(PGA) function. Median and 95% confidence level curves are shown. Two earthquake scenarios defined by PGA values of 0.11 g and 0.24 g are also depicted.

In **Procedure B** the uncertainties in the mechanical properties are considered in the construction of the fragility curves and the uncertainties in the seismic actions are considered in the obtaining of Sd_p, therefore the function $DI(Sd_p)$ takes into account both sources of uncertainty. The **procedure A** is used in the following as an application example. Sd_p values are taken from the Sd_p(PGA) function in Fig. 21 considering median and upper 95% confidence values. These values are shown in Table 9. Fig. 22 shows the $DI(Sd_p)$ curve. This $DI(Sd_p)$ function, which has been obtained by using the median fragility curve and the median capacity spectrum, is assumed to be deterministic. The median and 95% upper confidence level Sd_p obtained in Fig. 21 are then used to get the corresponding DI values.

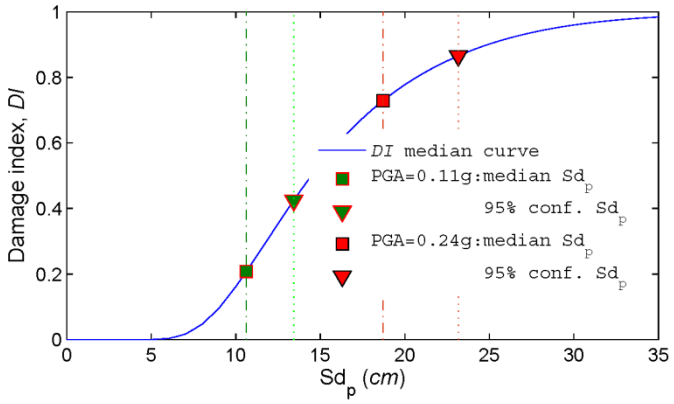

Fig. 22. $DI(Sd_p)$ function The median and 95% confidence Sd_p values, corresponding to PGA scenarios of 0.11g and 0.24 g are also shown.

Finally, the assumption of the binomial distribution of the probabilities of damage states allows computing the corresponding DPM. Table 9 summarizes the obtained results and Fig. 23 shows the corresponding DPM.

Table 9 Median and 95% upper confidence level values of Sd_p, DI and di, and DPM for two selected earthquake scenarios.

	EARTHQUAKE SCENARIO FOR PGA=0.11 g								
	Sd_p (cm)	DI	di	$P(ds_0)$	$P(ds_1)$	$P(ds_2)$	$P(ds_3)$	$P(ds_4)$	P_{TOT}
median val.	10.6	0.21	0.84	0.39	0.42	0.16	0.03	***	1.00
95% conf.	13.4	0.42	1.68	0.11	0.32	0.36	0.18	0.03	1.00
	EARTHQUAKE SCENARIO FOR PGA=0.24 g								
	Sd_p (cm)	DI	di	$P(ds_0)$	$P(ds_1)$	$P(ds_2)$	$P(ds_3)$	$P(ds_4)$	P_{TOT}
median val.	18.7	0.73	2.92	0.01	0.06	0.23	0.42	0.28	1.00
95% conf.	23.2	0.86	3.44	***	0.01	0.08	0.35	0.56	1.00

(***) means very low probability.

Thus the probabilistic approach allows obtaining results for whichever confidence level and it produces information which is richer and more useful for civil protection stakeholders and for decision makers, who may establish and choose the preferred levels of security. As a special case, note in Table 9 and in Fig. 23 how for the 0.24 g earthquake scenario the median and the 95% confidence level probabilities of the damage state *Complete*, $P(ds_4)$, are respectively of 28% and 56%, thus indicating a great uncertainty of this critical value, which is fundamental for estimating other sensitive and crucial quantities as, for instance, the numbers of expected casualties and homeless people.

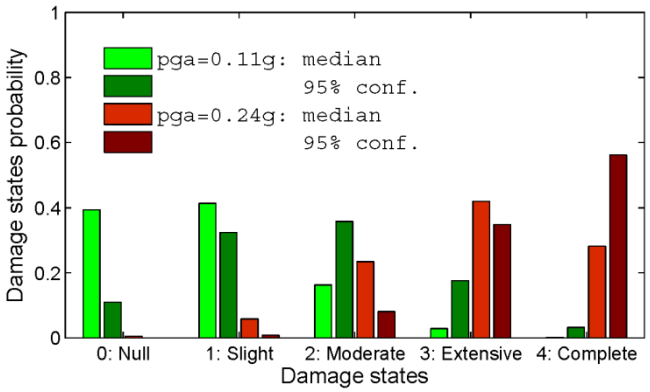

Fig. 23 DPM for PGA=0.11 g and 0.24 g. Median values and 95% upper confidence levels are shown.

There is not a standard procedure to realize seismic risk assessment in a probabilistic way. The best procedure depends on the quantity and quality of the

information available. Uncertainties must be carefully analyzed and should be taken into account in an adequate way. Low demanding scenarios may not be critical, as the influence of the uncertainties is lower but, for the analysis of intermediate and high demanding scenarios this fact may be crucial. When the quantity and quality of the data is adequate, a suitable straightforward way to conduct such studies can be as follows: **Step 1**: use a probabilistic approach to obtain Sd_p values corresponding to the confidence levels that are required; PA-8 procedure can be sufficient. **Step 2**: use deterministic values of the parameters of the building to get capacity curves, fragility curves and the $DI(Sd_p)$ function; in this step different assumptions can be adopted depending on the features of the actual buildings. For instance, mean, increased and decreased values of the mechanical properties of the materials or of other variables involved in the design and construction of the buildings can be used respectively for low-code, high-code and no-code buildings. **Step 3**: determine DI and DPM for the required Sd_p values. Obviously, other methods based on the **Procedure B** can be used. In any case it is important to not take into account the uncertainties more than once and to make the adequate choice to not overestimate or underestimate the uncertainties involved in the seismic actions and in the mechanical and geometrical properties of the structure.

7 Conclusions

The main conclusions of this work are: 1) for low-to-moderate earthquakes, simplified deterministic NLSA can lead to quite good results when compared to more sophisticated NLDA; and 2) uncertainties in the input variables lead to significant uncertainties into the structural response and expected damage. These two main conclusions are described in more detail in the following. Concerning the comparison of NLSA and NLDA, by using a deterministic model and characteristic values of the involved parameters we conclude that, for the building analyzed herein and for small-to-intermediate earthquakes, NLSA leads to fairly good results, although they are somewhat conservative. PA-8 procedure leads to more realistic results when compared to NLDA. The EDA technique is very straightforward but may lead to quite conservative results and, therefore, the PA-8 technique should be preferred. Furthermore, for intense seismic actions, to use

NLDA is justified. However, note that NLSA is on the safety side. The probabilistic analyses confirm these conclusions. Concerning the influence that the uncertainties of the properties of the materials and those of the seismic actions have on the uncertainties in the structural response, the main conclusions are outlined as follows. 1) All the results obtained with simplified and sophisticated structural analysis procedures show significant uncertainties in the computed output variables. It is important to observe that the coefficients of variation of the input variables used in this work are relatively small. 2) The correlation matrix between input and output variables provides valuables insights that can be useful not only in the design of new structures but also in the seismic risk assessment of existing ones. 3) The uncertainties in the response increase with the increase of the seismic actions due to the nonlinear behavior of the structural response; thus, the uncertainties in the capacity spectra increase with the spectral displacement and uncertainties in the fragility curves increase with the damage state. 4) The major influence in the randomness of the structural response of the buildings comes from the randomness of the seismic action; however the influence of the uncertainties in the mechanical properties of the materials is also significant. 5) The use of characteristic values in deterministic simplified approaches does not assure that the confidence level of the response be similar to that of the input variables. This fact is attributed to the nonlinear behavior of the structural system and it is evidenced by the significant differences between the expected damage obtained by means of deterministic and probabilistic NLDA. Specifically, the expected damage index obtained with the deterministic approach may become 20% lower than the expected damage index obtained with the probabilistic approach. Finally, it is important to remark that, regardless of the methodology, when assessing seismic vulnerability, it is crucial to follow an approach that takes into account the nonlinear behavior of the structure, the randomness of the mechanical properties of materials and the uncertainties associated with the seismic inputs.

Acknowledgements: The thoughtful comments and suggestions of Julian J. Bommer helped us to address the probabilistic treatment of the seismic actions and to improve the manuscript. The thorough review of two anonymous referees is also acknowledged. Special thanks are given to Emilio Carreño and Juan M. Alcalde of the Instituto Geográfico Nacional (IGN) who provided us the Spanish accelerogram database. M. Mar Obrador has carefully revised the English. This work has been partially funded by the Spanish government and the European Commission with FEDER

funds through research projects CGL2008-00869/BTE, CGL2011-23621, CGL2011-29063INTERREG: POCTEFA 2007-2013/ 73/08 and MOVE-FT7-ENV-2007-1-211590. Yeudy F. Vargas has a scholarship from an IGC-UPC joint agreement.

References

Ambraseys N, Smit P, Sigbjornsson R, Suhadolc P, Margaris B (2002) Internet-Site for European Strong-Motion Data. European Commission, Research-Directorate General, Environment and Climate Programme http://wwwisesdhiis/ESD_Local/framesethtm (last accesed 2011-04-17)

Ambraseys N, Smit P, Douglas J, Margaris B, Sigbjornsson R, Olafsson S, Suhadolc P, Costa G (2004) Internet-Site for European Strong-Motion Data. Bollettino di Geofisica Teorica ed Applicata 45 (3): 113-129

ATC (1985) ATC-13. Earthquake damage evaluation data for California. Applied Technology Council. Redwood City, California USA

ATC (1991) ATC-25. Seismic Vulnerability and impact of disruption of lifelines in the conterminous United States. Applied Technology Council. Funded By Federal Emergency Management Agency. ATC Redwood City. California

ATC (1996) ATC-40. Seismic evaluation and retrofit of concrete buildings. Applied Technology Council. Redwood City. California

Barbat A H, Mena U, Yépez F (1998) Evaluación probabilista del riesgo sísmico en zonas urbanas Revista internacional de métodos numéricos para cálculo y diseño en ingeniería, 14 (2): 247-268

Barbat A H, Yépez F, Canas JA (1996) Damage scenarios simulation for risk assessment in urban zones, Earthquake Spectra 2 (3): 371-394

Barbat AH, Pujades LG, Lantada N, Moreno R (2008) Seismic damage evaluation in urban areas using the capacity spectrum method: application to Barcelona. Soil Dynamics and Earthquake Engineering, 28:851–865

Bommer JJ, Crowley H (2006) The influence of ground motion variability in earthquake loss modelling, Bulletin of Earthquake Engineering 4 (3): 231-248

Borzi B, Phino R, Crowley H (2008) Simplified Pushover analysis for large-scale assessment of RC buildings. Engineering Structures 30:804-820

Carr AJ (2000) Ruaumoko-Inelastic Dynamic Analisys Program. Dept of Civil Engineering Univ of Canterbury. Christchurch. New Zealand

Chopra AK, Goel RK (1999) Capacity-Demand-Diagram Methods based on Inelastic Design Spectrum. Earthquake spectra 15 (4):637-656

Crowley H, Bommer JJ, Pinho R, Bird JF (2005) The impact of epistemic uncertainty on an earthquake loss model. Earthquake Engineering and Structural Dynamics 34 (14):1635-1685

Dolsek M (2009) Effects of uncertainties on seismic response parameters of reinforced concrete frame. Safety, Reliability and Risk of Structures, Infrastructures and Engineering Systems. Proceedings of the 10th International Conference on Structural Safety and Reliability,

ICOSSAR, 13-17 September 2009, Osaka, Japan, Edited by Hitoshi Furuta, Dan M Frangopol, and Masanobu Shinozuka, Pages 653-660, CRC Press

EC8 (2004) EN-1998-1. Eurocode 8: Design of structures for earthquake resistance -Part 1 General rules, seismic actions and rules for buildings English version

Faccioli E (2006) Seismic hazard assessment for derivation of earthquake scenarios in Risk-UE. Bull Earthq Eng 4:341–364

Faccioli E, Pessina V(2003) WP2–Basis of a handbook of earthquake ground motions scenarios, Risk-UE project WP-2 report

Fajfar P (1999) Capacity spectrum method based on inelastic demand spectra. Earthquake Engineering and Structural Dynamics 28:979-993

Faleiro J, Oller S, Barbat AH (2008) Plastic-damage seismic model for reinforced concrete frames, Computers and Structures 86 (7-8):581-597

FEMA (1997) NEHRP guidelines for the seismic Rehabilitation of buildings. FEMA 273 and NEHRP Commentary on the Guidelines for Seismic Rehabilitation of Buildings, FEMA 274. Federal Emergency Management Agency, Washington DC

FEMA (19979 Earthquake Loss Estimation Methodology, HAZUS'99 (SR 2) Technical Manual, Federal Emergency Management Agency. Washington DC

Fragiadakis M, Vamvatsikos D (2010) Estimation of Uncertain Parameters using Static Pushover Methods. In Proceedings of the tenth international conference on structural safety and reliability (icossar2009), osaka, japan, 13–17 september 2009 Safety Reliability and Risk of Structures, Infrastructures and Engineering Systems Furuta H, Frangopol DM and M Shinozuka Eds Taylor and Francis Group, London, UK. 659-660

Freeman SA (1978) Prediction of response of concrete buildings to severe earthquake motion Publication SP-55, American Concrete Institute, Detroit, MI, 589-605

Freeman SA (1998) Development and use of capacity spectrum method. Proceedings of the 6th US national conference on earthquake engineering, Seattle, CD-ROM, EERI

Freeman SA, Nicoletti JP, Tyrell JV (1975) Evaluations of existing buildings for seismic risk--a case study of Puget Sound Naval Shipyard, Bremerton,Washington Proceedings of the 1st US national conference on earthquake engineering, Oakland, California, 113–122

Gasparini D, Vanmarcke EH (1976) Simulated earthquake motions compatible with prescribed response spectra. MIT Department of Civil Engineering Research report R76-4, Order No 527

Grünthal G (1998) European Macroseismic Scale 1998 EMS-98. Conseil de L'Europe Cahiers du centre Européen de Géodynamique et de Séismologie 15

Hancock J, BommerJJ (2006) A state of knowledge Review of the influence of strong motion duration on structural damage. Earthquake Spectra 22(3): 827-845

Hancock J, Bommer JJ, Stafford PJ (2008) Numbers of scaled and matched accelerograms required for inelastic dynamic analyses. Earthquake Engineering and Structural Engineering 37(14):1585-1607

Hou S (1968) Earthquake simulation models and their applications, MIT Department of Civil Engineering Research Report R68-17

Kalos M, Whitlock PA (1986) Monte Carlo Methods. Volume I: Basics. Wiley\&Sons

Kim SP, Kuruma YC (2008) An alternative pushover analysis procedure to estimate seismic displacement demands Engineering structures 30:3793-3807 (2008)

Lagomarsino S, Giovinazzi S (2006) Macroseismic and mechanical models for the vulnerability and damage assessment of current buildings. Bull Earthq Eng 4:415–443

Lantada N, Pujades LG, Barbat AH (2009) Vulnerability index and capacity spectrum based methods for urban seismic risk evaluation: a comparison. Natural Hazards 51:501-524

Mahaney JA, Paret TF, Kehoe BE, Freeman SA (1993) The capacity spectrum method for evaluating structural response during the Loma Prieta earthquake. National earthquakes conference, Memphis

Mata PA, Oller S, Barbat AH (2007) Static analysis of beam structures under nonlinear geometric and constitutive behaviour. Computer Methods in Applied Mechanics and Engineering 196:4458-4478

McGuire RK (2004) Seismic hazard and risk analysis, Earthquake Engineering Research Institute, MNO-10

Milutinovic ZV, Trendafiloski GS (2003) WP04 Vulnerability of current buildings RISK-UE project of the EC: an advanced approach to earthquake risk scenarios with applications to different European towns

Mwafy AM and AS Elnashai AS (2001) Static pushover versus dynamic collapse analysis of RC buildings, Engineering Structures 23:407–424

NCSE-02 (2002) Real Decreto 997/2002, de 27 de septiembre, por el que se aprueba la norma de construcción sismorresistente: parte general y edificación (NCSR-02) Ministerio de Fomento Fecha de publicación: 11-10-2002 BOE: 244-2002: 35898-35966

Otani S (1974) Inelastic analysis of RC frames structures, J Struct Div, ASCE 100(7):1433–1449

Poursha M, Khoshnoudian F, Moghadam AS (2009) A consecutive modal pushover procedure for estimating the seismic demands of tall buildings. Engineering Structures 31:591-599

Pujades LG, Barbat AH, González-Drigo JR, Avila J, Lagomarsino S (2012) Seismic performance of a block of buildings representative of the typical construction in the Eixample district in Barcelona (Spain). Bulletin of Earthquake Engineering 10:331–349

Risk-UE (2004) An advanced approach to earthquake risk scenarios with applications to different European towns Contract number: EVK4-CT-2000-00014 Project of the European Commission

Satyarno I (1999) Pushover analysis for the seismic assessment of reinforced concrete buildings. Doctoral Thesis, Department of civil engineering, University of Canterbury. New Zealand

SEAOC Vision 2000 Committee (1995) Performance-Based Seismic Engineering. Report prepared by Structural Engineers Association of California, Sacramento, California Sacramento, CA April 1995 final report

Vamvatsikos D, Cornell CA (2001) The Incremental Dynamic Analysis, Earthquake Engineering and Structural Dynamics, 31(3): 491-514

Vargas YF, Pujades LG, Barbat AH, Hurtado JE (2010) Probabilistic Assessment of the Global Damage in Reinforced Concrete Structures. Proceeding of the 14th European Conference on Earthquake Engineering, Ohrid August 2010

Vielma JC, Barbat AH, Oller S (2009) Seismic performance of waffled-slabs floor buildings. Structures and Buildings (Proceedings of the Institution of Civil Engineering), 162(SB3):169-182

Vielma JC, Barbat AH, Oller S (2010) Seismic safety of limited ductility buildings. Bulletin of Earthquake Engineering 8(1):135-155

Vitruvius (1 BC) The ten books on architecture. Translated by MH Morgan Cambridge Harvard University Press, 1914

Appendix

Accelerograms used in NLDA

NLDA requires accelerograms. Stochastic analyses require a significant number of accelerograms, all of them well-matched with a target spectrum. So, given a target response spectrum and a specific database of acceleration records, the procedure used in this article for selecting accelerograms is the following. **Step 1**: normalize the target spectrum at the zero period. **Step 2**: compute the corresponding normalized spectrum for each accelerogram. **Step 3**: compute a measure of the misfit between the computed and target spectra; in this case, this measure is the error computed according to the following equation:

$$\varepsilon_j = \frac{1}{n-1}\sqrt{\sum_{i=1}^{n_j}\left(y_{ji} - Y_i\right)^2} \quad j = 1\cdots N, \qquad i = 1\cdots n \tag{8}$$

where ε_j is a least square measure of the misfit between the spectrum of the accelerogram *j* and the target spectrum; $y_{i,j}$ is the spectral ordinate *i* of the spectrum of the accelerogram *j*, and Y_i is the corresponding *i* ordinate of the target spectrum; *n* is the number of spectral ordinates of the accelerogram, assumed to be the same for each accelerogram *j*, and *N* is the number of accelerograms. **Step 4**: organize the spectra according increasing errors. **Step 5**: let $Sa_{ik}\ i = 1\cdots n, k = 1\cdots N$, be the *i*-th spectral ordinate corresponding to the spectrum of the accelerogram *k*, once the accelerogram series has been arranged in such a way that $\varepsilon_k \le \varepsilon_{(k+1)} \quad k = 1\cdots N-1$. Compute the following new spectra:

$$b_{im} = \frac{1}{m}\sum_{k=1}^{m} Sa_{ik} \qquad i = 1\cdots n, \quad m = 1\cdots N; \tag{9}$$

b_{im} are now the spectral ordinates of the mean of the first *m* spectra, once they have been arranged. **Step 6**: compute the following new error function (Er_m), which is similar to that given in equation (9).

$$Er_m = \frac{1}{n-1}\sqrt{\sum_{i=1}^{n_m}\left(b_{im} - Y_i\right)^2} \quad m = 1\cdots N, \quad i = 1\cdots n \tag{10}$$

The value of *m* that minimizes the value of Er_m is considered as the optimum number of accelerograms that are compatible with the given target spectrum and

that can be used of the given database. Of course, the value of Er_1 is also crucial for knowing the goodness of the fit. For databases with a large number of accelerograms, Er_1 is really small while we found m values of several tens. Some additional basic assumptions can be taken in order to reduce the size of the database. Information about the magnitude and focal mechanism of the earthquakes and about distance and soil type of the accelerometric stations can be used to significantly reduce the number of acceleration records to be tested. This procedure has been applied to the European (Ambraseys et al. 2002; 2004) and Spanish strong motion databases. As the European database is larger, most of the selected accelerograms are taken from this database but for spectra type 2, some accelerograms of the Spanish database were selected too. For each spectrum, 1A, 1D, 2A and 2D, more than 1000 records of acceleration were tested. Table 10 shows the statistics of the distributions of the magnitudes of the events corresponding to the accelerograms selected compatibles with the 1A, 1D, 2A and 2D spectra. Fig. 24 shows the error function, Er_m in equation (11), for the EC8 1D spectrum. The value of m minimizing this function has been found to be 20.

Table 10 Statistics: mean values, standard deviations and coefficients of variation of the magnitudes of the earthquakes corresponding to the selected accelerograms and spectra.

EC8 spectrum type	Mean value (μ_M)	Standard deviation (σ_M)	Coef. of var. *c.o.v.*
1A	5.5	1.22	0.20
1D	6.5	0.72	0.11
2A	5.3	0.82	0.16
2D	5.2	0.99	0.19

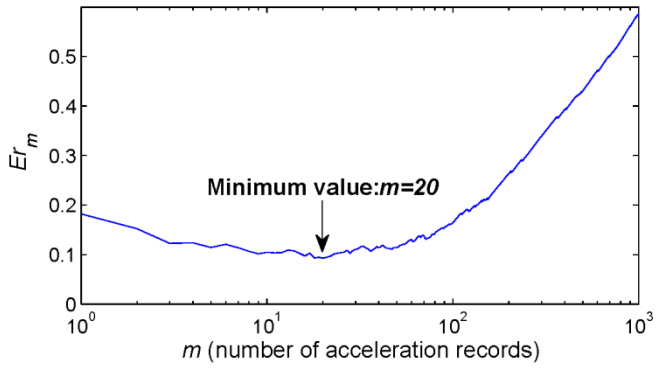

Fig. 24 Function Er_m used to optimize the number of compatible accelerograms. This example corresponds to the Eurocode EC8, 1D spectrum and m=20. The main parameters of the selected records are shown in Table 11.

Table 11 shows the main parameters of these accelerograms. The mean values of the magnitude, distance and depth are respectively 6.5, 67 km and 16.7 km and the corresponding standard deviations are 0.7, 53.6 km and 17.6 km. Fig. 25a shows the target EC8 1D spectrum, the mean spectrum and the spectrum defined by the median values plus one standard deviation. The fundamental period of the building is also plotted in this figure. Fig. 25b shows an example of compatible accelerogram.

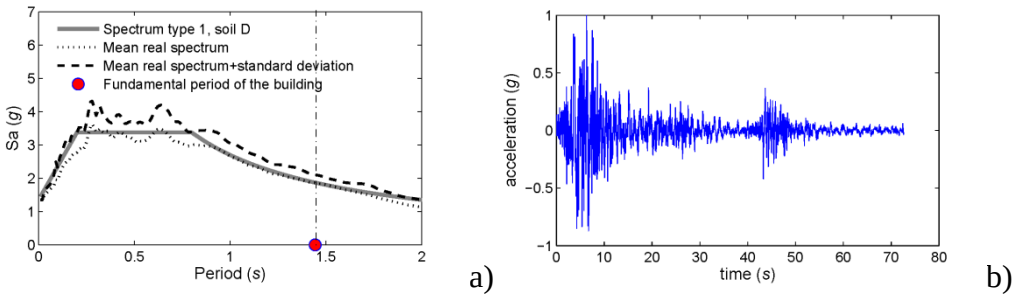

Fig. 25 a) Normalized EC8 1D spectrum. The mean and the mean plus one standard deviation spectra are also shown. The fundamental period of the structure is plotted too. b) Example of one accelerogram matching this spectrum.

Table 11 Main parameters of the accelerograms compatible with the EC81D spectrum.

event n.	Date	Epicenter (deg) Lat N	Lon E	depth (km)	Mag.	M.type	Station name	Distance (km)
1	06.05.1976	46.32	13.32	6	6.3	Mw	Castelfranco-Veneto	132
2	06.05.1976	46.32	13.32	6	6.3	Mw	Codroipo	48
3	15.09.1976	43.32	13.16	12	5.9	Mw	Cortina d´Ampezzo	83
4	16.09.1978	33.36	57.42	5	7.3	Ms	Boshroyeh	55
5	15.04.1979	41.98	18.98	12	7.0	Ms	Ulcinj-Hotel Olimpic	24
6	23.11.1980	47.78	15.33	16	6.5	Mw	Bagnoli-Irpino	23
7	23.11.1980	47.78	15.33	16	6.5	Mw	Rionero in Vulture	33
8	23.11.1980	47.78	15.33	16	6.5	Mw	San Giorgio la Molara	64
9	17.01.1983	38.07	20.25	14	7.0	Ms	Agrinio-Town Hall	118
10	06.06.1986	38.01	37.91	11	5.7	Ms	Galbasi-Devlet Hastanesi	34
11	13.09.1986	37.10	22.18	8	5.7	Ms	Kalamalata-Prefecture	9
12	30.05.1990	45.85	26.66	89	6.8	Ms	Istrita	80
13	20.06.1990	39.96	49.41	19	7.3	Ms	Tehran-Sarif University	223
14	20.06.1990	39.96	49.41	19	7.3	Ms	Tonekabun	131
15	06.11.1992	38.16	27.00	17	6.0	Ms	Izmir-Bayindirlik	30
16	26.09.1997	43.02	12.89	7	5.7	Mw	Bevagna	25
17	09.11.1997	42.90	12.95	10	4.8	Mb	Castelmuovo-Assisi	31
18	23.11.1980	40.78	15.33	16	6.5	Mw	Gioia-Sannitica	94
19	17.08.1999	40.70	29.99	17	7.4	Mw	Bursa-Sivil Savunma	93
20	17.08.1999	40.70	29.99	17	7.4	Mw	Izmit-Metereoloji-Istasyonu	10